Available online at www.sciencedirect.com
SCIENCE DIRECT®
Journal of Magnetic Resonance 173 (2005) 209–217
JMR Journal of Magnetic Resonance
www.elsevier.com/locate/jmr

Effects of T_2-relaxation in MAS NMR spectra of the satellite transitions for quadrupolar nuclei: a ^{27}Al MAS and single-crystal NMR study of alum $KAl(SO_4)_2 \cdot 12H_2O$

Morten Daugaard Andersen, Hans J. Jakobsen, Jørgen Skibsted*

Department of Chemistry, Instrument Centre for Solid-State NMR Spectroscopy, University of Aarhus, DK-8000 Aarhus C, Denmark

Received 15 October 2004; revised 7 December 2004
Available online 22 January 2005

Abstract

Asymmetries in the manifold of spinning sidebands (ssbs) from the satellite transitions have been observed in variable-temperature ^{27}Al MAS NMR spectra of alum ($KAl(SO_4)_2 \cdot 12H_2O$), recorded in the temperature range from −76 to 92 °C. The asymmetries decrease with increasing temperature and reflect the fact that the ssbs exhibit systematically different linewidths for different spectral regions of the manifold. From spin-echo ^{27}Al NMR experiments on a single-crystal of alum, it is demonstrated that these variations in linewidth originate from differences in transverse (T_2) relaxation times for the two inner ($m = 1/2 \leftrightarrow m = 3/2$ and $m = -1/2 \leftrightarrow m = -3/2$) and correspondingly for the two outer ($m = 3/2 \leftrightarrow m = 5/2$ and $m = -3/2 \leftrightarrow m = -5/2$) satellite transitions. T_2 relaxation times in the range 0.5–3.5 ms are observed for the individual satellite transitions at −50 °C and 7.05 T, whereas the corresponding T_1 relaxation times, determined from similar saturation-recovery ^{27}Al NMR experiments, are almost constant ($T_1 = 0.07$–0.10 s) for the individual satellite transitions. The variation in T_2 values for the individual ^{27}Al satellite transitions for alum is justified by a simple theoretical approach which considers the cross-correlation of the local fluctuating fields from the quadrupolar coupling and the heteronuclear (^{27}Al–^{1}H) dipolar interaction on the T_2 relaxation times for the individual transitions. This approach and the observed differences in T_2 values indicate that a single random motional process modulates both the quadrupolar and heteronuclear dipolar interactions for ^{27}Al in alum at low temperatures.

Keywords: Quadrupolar nuclei; Satellite transitions; Transverse relaxation; Quadrupolar coupling; Dipolar interaction

1. Introduction

Magic-angle spinning (MAS) NMR of the satellite transitions for half-integer spin quadrupolar nuclei, generating a complete manifold of spinning sidebands (ssbs), has proven to be a strong tool for determination of the quadrupole coupling parameters (C_Q and η_Q) for small and intermediate quadrupole couplings [1,2]. For spin nuclei that are only influenced by the quadrupole coupling interaction, the MAS NMR spectrum exhibits a manifold of ssbs from the satellite transitions, which is symmetric around the central transition when the spectrum is recorded under optimum experimental conditions. However, small variations in ssb linewidths may be observed throughout the ssb manifold as a result of the difference in second-order quadrupolar broadening for the individual satellite transitions [3,4]. Asymmetries in the ssb manifold from the satellite transitions may arise from internal as well as external effects. The internal effects include chemical shift anisotropy (CSA), which results in distinct asymmetries of the ssb intensities that additionally allow determination of the CSA parameters and the relative orientation of the CSA and quadrupole coupling tensors [5]. The external effects

* Corresponding author. Fax : +45 8619 6199.
E-mail address: jskib@chem.au.dk (J. Skibsted).

1090-7807/$ - see front matter © 2004 Elsevier Inc. All rights reserved.
doi:10.1016/j.jmr.2004.12.002

include small deviations from exact magic-angle setting, which may lead to unique lineshapes for the individual ssbs [6]. Furthermore, RF offsets caused by improper cable lengths for the $\lambda/4$ cable in the duplexer of the preamplifier and between the probe and the preamplifier (and/or filters in this line) may give a "tilt" of the ssb manifold [7,8]. However, optimization of these external effects (magic-angle and cable lengths) can generally result in a highly symmetric MAS spectrum, if the nucleus under investigation is influenced only by the quadrupole coupling interaction.

In this work, we report the observation of an internal effect that has not been considered earlier and which may result in asymmetries of the manifold of ssbs from the satellite transitions. This effect is related to differences in ^{27}Al ($I = 5/2$) transverse (T_2) relaxation times for the two inner transitions ($m = 1/2 \leftrightarrow m = 3/2$ and $m = -1/2 \leftrightarrow m = -3/2$) and correspondingly for the two outer transitions ($m = 3/2 \leftrightarrow m = 5/2$ and $m = -3/2 \leftrightarrow m = -5/2$), which are observed in ^{27}Al MAS NMR spectra of the satellite transitions for the alum $KAl(SO_4)_2 \cdot 12H_2O$, recorded at temperatures in the range -76 to 92 °C. The variation in T_2 values for the different satellite transitions is elucidated by consideration of the effects from the fluctuating fields from the quadrupolar interaction and the ^{27}Al–^{1}H dipolar couplings on the T_2 relaxation. The effects of cross-correlation of anisotropic interactions such as CSA–dipole, dipole–dipole, and quadrupole–dipole cross-correlation have been observed and described in detail for transverse relaxation of coupled spins in the liquid-state [9]. An important application of cross-correlation is achieved in the TROSY experiment which utilizes the cross-correlation of CSA and dipolar interactions (^{1}H, ^{15}N, and ^{13}C) in structural determination of large biological molecules in solution [10]. Moreover, the effect of quadrupole–dipole cross-correlation (^{2}H–^{13}C) on the lineshape for the ^{13}C resonance has been observed and evaluated theoretically for a ^{2}H-labelled protein in solution [11].

2. Experimental

The powder sample of alum ($KAl(SO_4)_2 \cdot 12H_2O$) was purchased from Merck (Darmstadt, Germany) and used without further purification. Large crystals of alum were obtained from an aqueous solution by slow evaporation at room temperature. A deuterated powder sample ($KAl(SO_4)_2 \cdot 12D_2O$) was prepared by dehydration of alum at 150 °C followed by recrystallization in D_2O at room temperature. This process was repeated three times and resulted in 94% deuteration, as estimated by ^{1}H MAS NMR. The basic structure and purity of the samples were confirmed by X-ray diffraction.

The ^{27}Al MAS and single-crystal NMR experiments were performed on a Varian *Unity* INOVA-300 (7.05 T) spectrometer using a homebuilt, narrow-bore, variable-temperature (VT) CP/MAS NMR probe for 7 mm o.d. rotors. The probe is capable of operating in the temperature range from -140 to 210 °C by regulation of the temperature for the air-bearing gas, employing a homebuilt VT heater/controller unit as described elsewhere [12]. The temperature gradient across the rotor volume is less than 2 °C and the actual sample temperature was determined using ^{207}Pb MAS NMR of $Pb(NO_3)_2$ as a NMR thermometer [13]. For the MAS NMR experiments, slices of $NaNO_3$, packed above/below the sample of $KAl(SO_4)_2 \cdot 12H_2O$ in the rotor, allowed an accurate adjustment (if necessary) of the magic angle at each temperature by minimization of the linewidths observed for the ^{23}Na satellite transitions. The ^{27}Al VT MAS NMR experiments employed single-pulse excitation with a pulse width of 1.0 μs for a RF field strength of $\gamma B_1/2\pi = 40$ kHz, ^{1}H decoupling ($\gamma B_2/2\pi = 45$ kHz), a relaxation delay of 2 s, and a spinning speed of $\nu_r = 3.0$ kHz regulated to ± 1 Hz by the Varian spinning-speed controller. The single-pulse ^{27}Al NMR experiments on the single crystal of alum used a pulse width of 1.0 μs for a RF field strength of $\gamma B_1/2\pi = 40$ kHz, ^{1}H decoupling ($\gamma B_2/2\pi = 50$ kHz), and a relaxation delay of 4 s. The crystal was packed in the middle of a 7 mm zirconia rotor with silica powder in the top and bottom of the rotor and the rotor was fixed in the probe for the VT experiments. The saturation-recovery ^{27}Al NMR experiments [14] used the same RF field strengths as the single-pulse spectra, 10 saturation pulses with a width of 4.5 μs and separated by a delay of 200 μs, and recovery delays in the range 1.0 ms to 0.5 s. The spin-echo ^{27}Al NMR experiments used high-power ^{1}H decoupling ($\gamma B_2/2\pi = 45$ kHz) but a low RF strength ($\gamma B_1/2\pi \approx 2.6$ kHz) for the selective $\pi/2$ and π pulses with pulse widths in the range 36–53 μs and 72–106 μs, respectively. For each transition, the pulse widths for the $\pi/2$ and π pulses were optimized on the alum crystal for the fixed RF field strength. Moreover, the spin-echo NMR experiments employed echo delays in the range $\tau = 25$–3000 μs and a relaxation delay of 4 s. Simulations of the solid-state ^{27}Al MAS NMR spectra were performed on a SUN ULTRA 5 workstation using the *STARS* solid-state NMR software package [2,5]. ^{27}Al isotropic chemical shifts are in ppm relative to an external sample of 1.0 M $AlCl_3 \cdot 6H_2O$.

3. Results and discussion

$KAl(SO_4)_2 \cdot 12H_2O$ belongs to the large family of isotypic compounds called alums, $A^{+}B^{3+}(RO_4)_2 \cdot 12H_2O$; A = Na, K, NH_4, Rb, Cs, and Tl; B = Al, Ga, and Cr; R = S, Se. The crystal structures of alums may be

divided into three subtypes, α-, β-, and γ-alums [15], with the same space group (cubic, *Pa*3), which are distinguished by the arrangements of the RO_4^{2-} anions and the water molecules in the lattice. The crystal structure of the α-alums, which includes $KAl(SO_4)_2 \cdot 12H_2O$ [16], is characterized by a $B(H_2O)_6^{3+}$ octahedron, which is slightly distorted in the direction of one of the threefold axes, and RO_4^{2-} tetrahedra that are nearly symmetric with the central atom and one of the oxygens located on a threefold axis. The second coordination sphere of the B^{3+} ion contains six RO_4^{2-} tetrahedra which form a cavity for the $B(H_2O)_6^{3+}$ octahedron. Thus, the crystal symmetry of $KAl(SO_4)_2 \cdot 12H_2O$ entails an axially symmetric ^{27}Al quadrupole coupling tensor and that the ^{27}Al–^{1}H dipolar and ^{27}Al quadrupolar tensors should be coincident.

The ^{27}Al MAS NMR spectra of the satellite transitions for alum ($KAl(SO_4)_2 \cdot 12H_2O$), recorded at three different temperatures and illustrated in Fig. 1, reveal significant asymmetries in the manifold of ssbs for the spectra recorded at low (−33 °C) and room temperature. Similar spectra recorded at other temperatures in the range −76 to 92 °C show that these asymmetries decrease with increasing temperature (T), resulting in a symmetric manifold of ssbs at high temperature ($T = 81$ °C, Fig. 1C). Examination of the ssb linewidths in the low-temperature spectra demonstrates that the asymmetries originate from a systematic variation in linewidths for the individual ssbs. For example, the ssbs of the inner singularities (“horns”), which originate mainly from the inner satellite transitions, exhibit linewidths of FWHM = 294 Hz and FWHM = 170 Hz for the horns at 30 and −30 kHz, respectively, in the ^{27}Al MAS NMR spectrum recorded at −33 °C. The insets in Fig. 2A illustrate that similar variations in ssb linewidths are also observed in spectral regions dominated by the outer satellite transitions. However, integration of the individual ssb intensities in the experimental spectrum recorded at −18 °C results in the stick-plot of ssb intensities in Fig. 2B, which is highly symmetric around the central transition. This demonstrates that the asymmetries do not arise from ^{27}Al chemical shift anisotropy. Furthermore, an examination of the linewidths for the central transition and the ssbs from the satellite transitions as a function of the ^{1}H decoupling RF field strength shows that the linewidths for each transition decrease for increasing decoupling field strengths up to $\gamma B_2/2\pi \approx 40$ kHz, whereas the linewidths remain constant for field strengths in the range $\gamma B_1/2\pi = 40$–100 kHz. Thus, the asymmetries in the ssb manifold do not arise from insufficient ^{1}H decoupling.

Least-squares optimization to the integrated ssb intensities (Fig. 2B) results in the parameters, $C_Q = 342$ kHz, $\eta_Q = 0.00$, and $\delta_{iso} = 0.7$ ppm and the simulation in Fig. 2C, which excellently reproduce the stick-plot of experimental ssb intensities. A similar analysis of 14 VT ^{27}Al MAS NMR spectra recorded in the temperature range from −76 to 92 °C shows that the quadrupole coupling constant (Fig. 3) and the isotropic chemical shift (δ_{iso}, not shown) exhibit a linear temperature dependency, at least for this temperature range, whereas $\eta_Q = 0.00 \pm 0.05$ for all temperatures. Obviously, this observation for η_Q is in accord with the location of the Al^{3+} ion on a threefold axis in the crystal structure [16]. Linear regression analysis of the C_Q and δ_{iso} values as a function of temperature gives the equations

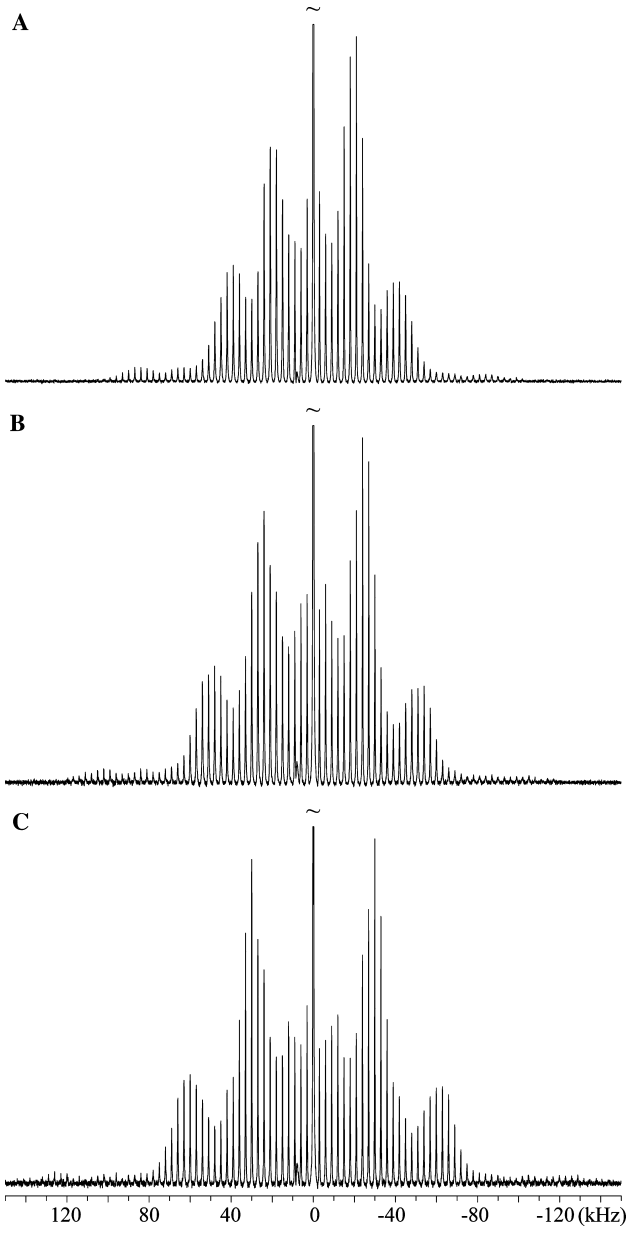

Fig. 1. ^{27}Al MAS NMR spectra (7.05 T) of the manifold of ssbs from the satellite transitions for alum ($KAl(SO_4)_2 \cdot 12H_2O$) recorded at (A) $T = -33$ °C, (B) $T = 25$ °C, and (C) $T = 81$ °C, employing ^{1}H decoupling and a spinning speed of $\nu_r = 3.0$ kHz.

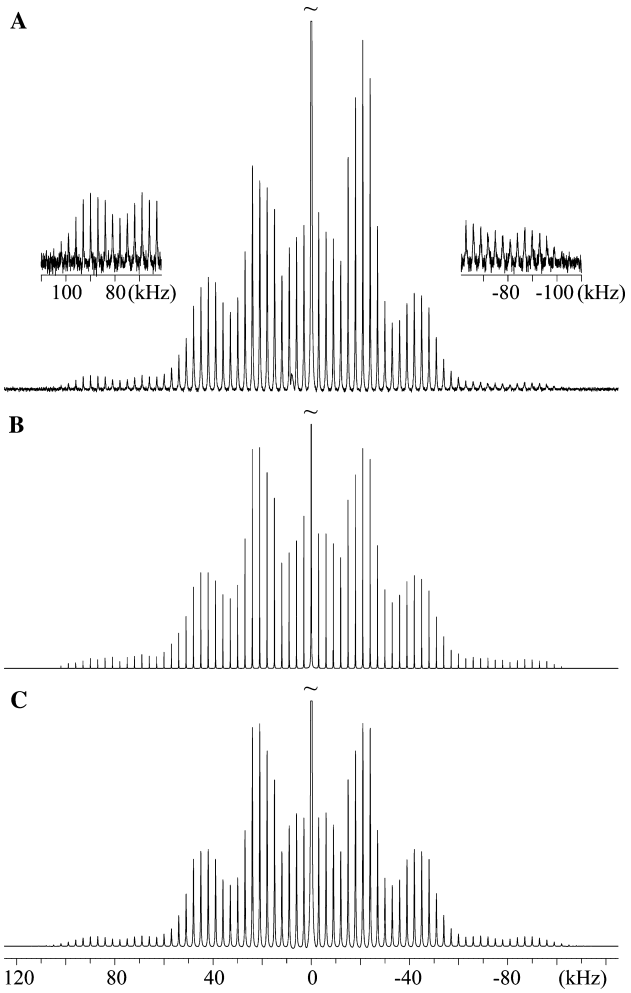

Fig. 2. (A) Experimental ^{27}Al MAS NMR spectrum (7.05 T, $\nu_r = 3.0$ kHz) illustrating the manifold of spinning sidebands from the satellite transitions for alum at $T = -18$ °C. (B) Stick-plot of integrated ssb intensities for the manifold in (A). (C) Optimized simulation of the manifold of ssbs in (B), employing the parameters $C_Q = 342$ kHz, $\eta_Q = 0.00$, and $\delta_{iso} = 0.7$ ppm. The insets in (A) display the ssbs of the outer regions of the manifold, using a vertical expansion by a factor of five, and illustrate that differences in ssb linewidth also are observed for the outer satellite transitions.

$$C_Q = 1.314\ (\text{kHz}/^\circ\text{C})T + 362\ \text{kHz}, \quad (1)$$

$$\delta_{iso} = 4.26 \times 10^{-3}(\text{ppm}/^\circ\text{C})T - 0.30\ \text{ppm} \quad (2)$$

with the correlation coefficients $R = 0.998$ and $R = 0.98$, respectively. The increase in C_Q with increasing temperature is in accord with an earlier single-crystal ^{27}Al NMR study of alum [17]. Several compounds of the alum family $(A^+B^{3+}(RO_4)_2 \cdot 12H_2O$; A = Na, NH_4, Rb, Cs; B = Al, Ga, Cr; and R = S, Se) have been investigated by multi-nuclear NMR and NQR by Weiden and Weiss [18–20]. For the α-alums (A = NH_4, Rb, B = Al, and R = S), they ascribe the positive temperature coefficient for $C_Q(^{27}\text{Al})$ to the possibility of the anisotropic vibrations for the Al^{3+} ion within the $Al(H_2O)_6^{3+}$ octahedron being larger than the vibrations

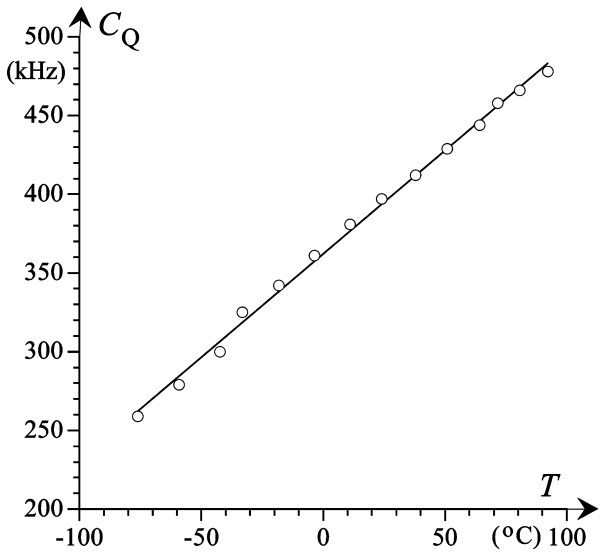

Fig. 3. Graph illustrating the temperature dependency of $C_Q(^{27}\text{Al})$ for alum in the temperature range from −76 to 92 °C. The straight line corresponds to the result of linear regression of the data given in Eq. (1).

of Al^{3+} in the cage of SO_4^{2-} ions. This result was achieved from point-monopole calculations of the temperature dependency for the ^{27}Al electric field gradient tensor [19,20].

The asymmetries of the ssb manifold in the ^{27}Al MAS NMR spectra (Figs. 1 and 2), which reflect variations in ssb linewidths, are ascribed to a difference in T_2 relaxation times for the individual transitions. Thus, employing the nomenclature of the energy-level diagram for a spin $I = 5/2$ nucleus given in Fig. 4, the two inner satellite transitions ($\nu(-\text{in})$ and $\nu(+\text{in})$) exhibit different T_2 values, and similarly for the two outer transitions ($\nu(-\text{out})$ and $\nu(+\text{out})$). To study the variation in T_2 values in more detail, a single-crystal of alum has been investigated at $T = -50$ °C. The cubic space group ($Pa3$) and the presence of four formula units in the unit cell [16] imply that resonances from four magnetically inequivalent ^{27}Al sites should be observed in the single-crystal ^{27}Al NMR spectrum. Since the ^{27}Al NMR spectra of the single crystal are obtained using a CP/MAS probe, a fixed orientation of the single crystal in the rotor was chosen which gave the best resolution of the 16 resonances, originating from the satellite transitions for the four magnetically inequivalent ^{27}Al sites. The ^{27}Al NMR spectrum ($T = -50$ °C) of the single crystal recorded under these conditions (Fig. 5) shows that resonances from the individual satellite transitions for the four magnetically different ^{27}Al sites are clearly resolved whereas the resonances from the central transitions cannot be distinguished. The resonances from the satellite transitions for the four different ^{27}Al sites are denoted **1**–**4** (Fig. 5) where the sign and subscript indicate the type of transition according to the energy-level

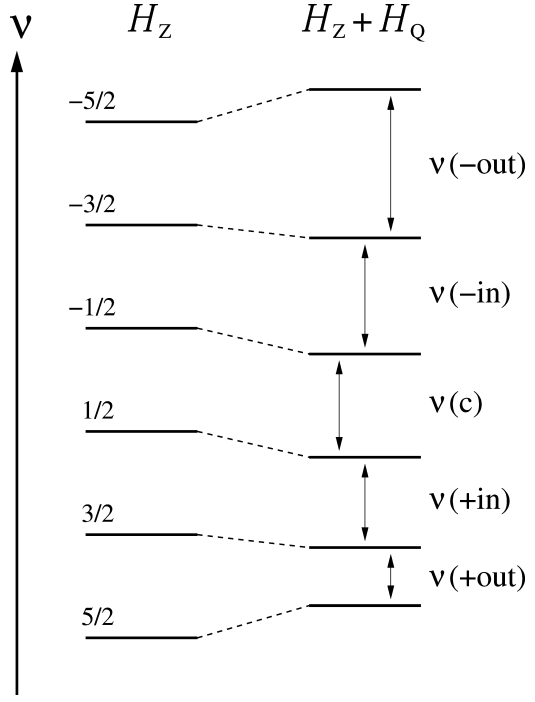

Fig. 4. Energy-level diagram for ^{27}Al illustrating the effect from the quadrupole interaction and defining the individual transitions, i.e., $\nu(-\text{out})$, $\nu(-\text{in})$, $\nu(+\text{in})$, and $\nu(+\text{out})$, used for the evaluation of the T_2 values.

diagram shown in Fig. 4 and the theoretical approach employed later (cf. Eq. (7)). From the spectrum of the single crystal and the linewidths listed in Table 1, it is apparent that the resonances from the individual satellite transitions for each ^{27}Al site exhibit different linewidths. For example, for ^{27}Al site **1**, the linewidths for the inner and outer satellites exhibit the ratios $\text{FWHM}(+\mathbf{1}_{\text{in}})/\text{FWHM}(-\mathbf{1}_{\text{in}}) = 1.6$ and $\text{FWHM}(+\mathbf{1}_{\text{out}})/\text{FWHM}(-\mathbf{1}_{\text{out}}) = 2.3$ (cf. Table 1).

The T_2 values are determined for the individual satellite transitions for the three ^{27}Al sites (**1**–**3**), which exhibit the largest dispersion in frequencies for these resonances, from spin-echo ^{27}Al NMR experiments employing soft $\pi/2$ and π pulses and spin-echo times in the range $25\ \mu\text{s} < \tau < 3.0$ ms. The pulse widths have been optimized for the individual resonances and the subsequent spin-echo ^{27}Al NMR experiments were performed on-resonance for each satellite transition. This

Table 1
^{27}Al T_2 relaxation times and linewidths for the individual satellite transitions in a single crystal of alum ($KAl(SO_4)_2 \cdot 12H_2O$) studied by ^{27}Al NMR (7.05 T) at $T = -50$ and 18 °C

Transition[a]	T_2 (ms)[c]	FWHM (Hz)[d]
$+\mathbf{1}_{\text{out}}$	0.76	674
$+\mathbf{1}_{\text{in}}$	0.99	500
$-\mathbf{1}_{\text{in}}$	2.08	312
$-\mathbf{1}_{\text{out}}$	3.53	296
$+\mathbf{2}_{\text{out}}$	0.53	967
$+\mathbf{2}_{\text{in}}$	0.71	659
$-\mathbf{2}_{\text{in}}$	1.71	350
$-\mathbf{2}_{\text{out}}$	1.90	370
$+\mathbf{3}_{\text{out}}$	0.57	811
$+\mathbf{3}_{\text{in}}$	0.74	541
$-\mathbf{3}_{\text{in}}$	1.63	355
$-\mathbf{3}_{\text{out}}$	0.97	490
$+\mathbf{4}_{\text{out}}$	—[e]	1000
$+\mathbf{4}_{\text{in}}$	—[e]	606
$-\mathbf{4}_{\text{in}}$	—[e]	500
$-\mathbf{4}_{\text{out}}$	—[e]	840
$+\mathbf{2}_{\text{out}}$[b]	0.59	749
$+\mathbf{2}_{\text{in}}$[b]	0.72	554
$-\mathbf{2}_{\text{in}}$[b]	1.47	360
$-\mathbf{2}_{\text{out}}$[b]	1.32	383

[a] The individual transitions are indexed according to the spectrum in Fig. 5 and the energy-level diagram in Fig. 4. The values are obtained at $T = -50$ °C if not otherwise stated.

[b] Data obtained at $T = 18$ °C for the same crystal orientation studied at $T = -50$ °C.

[c] The error limits for T_2 are estimated to ±0.05 ms for all transitions.

[d] Full width at half maximum (FWHM). The error limits are estimated to ±5 Hz for all transitions.

[e] Not determined (see text).

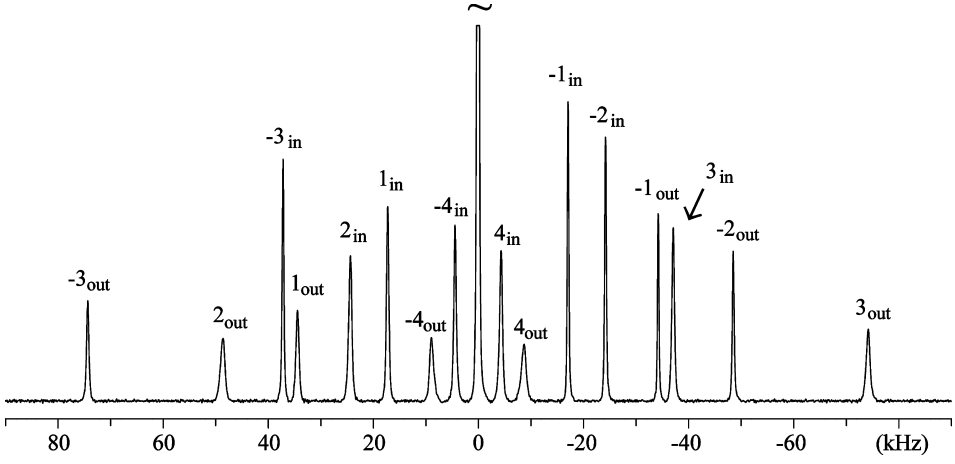

Fig. 5. ^{27}Al NMR spectrum (7.05 T, $T = -50$ °C) of a single crystal of alum recorded using high-power ^{1}H decoupling. The resonances from the satellite transitions for the four ^{27}Al sites are denoted **1**–**4** where the subscript indicates the type of satellite transition (cf. Fig. 4).

approach follows the results by Haase and Oldfield [21], who have shown that soft RF excitation with a pair of selective π/2 and π pulses gives the expected single-exponential spin-echo decay for half-integer spin-quadrupolar nuclei. However, a reliable determination of T_2 for the closely situated resonances from the satellite transitions for ^{27}Al site **4** could not be obtained in this manner. The plots in Fig. 6 of the normalized intensities as a function of the spin-echo time for the four satellite transitions for ^{27}Al site **1** reveal for each transition single-exponential relationships ($M(2\tau) = M_0\exp(-2\tau/T_2)$). However, minor oscillations in the intensities are observed for short spin-echo times. These oscillations may originate from components of the magnetization precessing at the quadrupole frequency as described earlier by Haase and Oldfield [21]. The graphs in Fig. 6 and the corresponding T_2 relaxation times (Table 1) clearly reveal that the two inner satellite transitions ($+\mathbf{1}_{in}$ and $-\mathbf{1}_{in}$) and similarly the two outer satellite transitions ($+\mathbf{1}_{out}$ and $-\mathbf{1}_{out}$) possess quite different T_2 relaxations times. Obviously, this variation is in accordance with the differences in linewidth (FWHM), observed for the individual transitions (Table 1), which exhibit an inverse proportionality with the T_2^* relaxation time (FWHM $= 1/(\pi T_2^*)$). From the relationship, FWHM $= 1/(\pi T_2) + W$, and the data in Table 1, values for the inhomogeneous broadening (W, i.e., magnetic field inhomogeniety) of $W = 200$, 236, and 171 Hz are determined for ^{27}Al sites **1**, **2**, and **3**, respectively. The variation in W may reflect the different orientations of the ^{27}Al sites **1**–**3** for the specific orientation of the single-crystal in the magnetic field. The T_2 values and linewidths determined for ^{27}Al sites **2** and **3** (Table 1) show

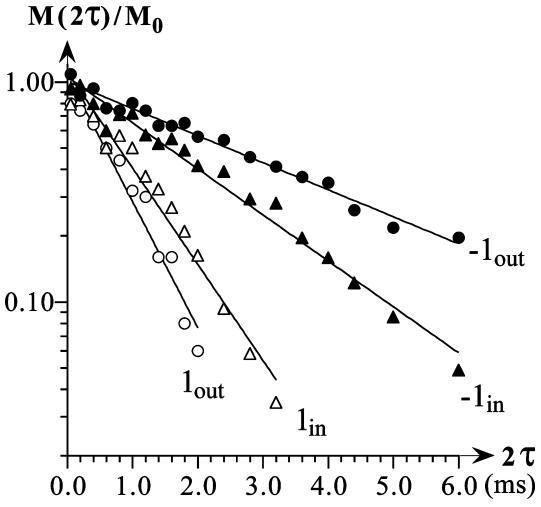

Fig. 6. Logarithmic plot of the intensities for the individual satellite transitions for ^{27}Al site **1**, observed in spin-echo ^{27}Al NMR spectra (7.05 T, $T = -50$ °C) of a single crystal of alum, as a function of the spin-echo time (2τ). The straight lines correspond to regression analysis, employing a single-exponential relationship for the decay of magnetization, and the T_2 values are listed in Table 1 for ^{27}Al site **1**.

a similar variation for the different transitions as observed for site **1**. Moreover, T_2 values and resonance linewidths have also been obtained at 18 °C for the ^{27}Al site **2** (Table 1). These data shows that the differences in T_2 and FWHM also are observed at ambient temperature. We note that the T_1 relaxation times have been determined for the alum crystal at −50 °C in a similar manner for the individual transitions from saturation-recovery ^{27}Al NMR experiments. However, the analysis of these spectra shows that the T_1 values are nearly identical for the individual transitions ($T_1 = 0.07$–0.10 s, $T = -50$ °C).

Woessner and Timken have investigated the influence of MAS on spin–lattice relaxation for the central transition of half-integer spin-nuclei with large quadrupole couplings [22]. They observed that the T_1 values determined from MAS NMR can be smaller as compared to those obtained from static-powder experiments because of spin exchange resulting from magnetic dipole–dipole interactions between nearby nuclei. A similar effect of MAS on the T_2 values for the satellite transitions cannot be excluded from the single-crystal experiments performed in this work. However, we note that ^{27}Al MAS NMR spectra of alum recorded using spinning speeds $\nu_r = 3.0$, 6.0, and 9.0 kHz all exhibit significant asymmetries in the manifold of spinning sidebands and differences in the ssb linewidths for the three spinning speeds, which indicate that the difference in T_2 values for the individual satellite transitions is not removed by MAS.

To our knowledge, the observation of different T_2 relaxation times for the individual satellite transitions of a half-integer spin quadrupole nucleus has not been reported before. An explanation for the variation in T_2 values may be obtained by a simple model which assumes that the T_2 relaxation results from the coupling of two fluctuating interactions. A similar approach has been used in an evaluation of the T_2 values for the forbidden transitions in the AX spin system to illustrate that information about the cross-correlation between two local fields can be achieved from these values [23]. For ^{27}Al in alum, the two fluctuating fields would be the quadrupole coupling and the heteronuclear (^{27}Al–^{1}H) dipolar interaction. Assuming the fluctuating fields from these interactions being simultaneously present, and for simplicity that the contribution from the dipolar term is a fluctuating local field in the z-direction, may result in the following fluctuating Hamiltonian:

$$H(t) = q(t)\left[I_z^2 - \frac{1}{3}I(I+1)\right] + d(t)I_z, \tag{3}$$

where $q(t)$ and $d(t)$ are the spatially dependent parts of the local fluctuating fields from the quadrupolar and dipolar interactions, respectively. The T_2 value for a single-quantum transition is given by $1/T_2 = \overline{(\Delta\omega_{m,m-1})^2}\tau_c$, where τ_c is the correlation time of the motion and

$\overline{(\Delta\omega_{m,m-1})^2}$ is the mean-square of $\Delta\omega_{m,m-1}(t)$. For the $m \leftrightarrow m-1$ transition, the Hamiltonian results in the fluctuating frequency

$$\Delta\omega_{m,m-1}(t) = (2m-1)q(t) + d(t). \quad (4)$$

If the terms $q(t)$ and $d(t)$ are not correlated, the mean-square of Eq. (4) gives the value

$$\overline{\Delta\omega^2_{m,m-1}} = (2m-1)^2\overline{q^2} + \overline{d^2}, \quad (5)$$

which will result in identical values of T_2 for the two inner satellite transitions and for the two outer satellite transitions. However, suppose the situation where $q(t)$ and $d(t)$ are correlated, for example in such a manner that the dipolar term can be expressed as $d(t) = kq(t)$ at all times, where k is a constant. In this case, the mean-square of Eq. (4) becomes

$$\overline{\Delta\omega^2_{m,m-1}} = (2m-1+k)^2\overline{q^2}, \quad (6)$$

resulting in the following different T_2 values for the five single-quantum transitions of the spin $I = 5/2$ nucleus:

$$\begin{aligned}
\frac{1}{T_2} &= (k+4)^2\overline{q^2}\tau_c \qquad 5/2 \leftrightarrow 3/2 \\
&= (k+2)^2\overline{q^2}\tau_c \qquad 3/2 \leftrightarrow 1/2 \\
&= k^2\overline{q^2}\tau_c \qquad 1/2 \leftrightarrow -1/2 \\
&= (k-2)^2\overline{q^2}\tau_c \qquad -1/2 \leftrightarrow -3/2 \\
&= (k-4)^2\overline{q^2}\tau_c \qquad -3/2 \leftrightarrow -5/2. \quad (7)
\end{aligned}$$

This predicted variation in T_2 values may explain the differences in the experimental values, observed for the different satellite transitions (Table 1), e.g., for Al site **1** it is observed that $T_2(+\mathbf{1}_{out}) < T_2(+\mathbf{1}_{in}) < T_2(-\mathbf{1}_{in}) < T_2(-\mathbf{1}_{out})$, cf. Table 1. Furthermore, the similarity in the variations of the T_2 values given by Eq. (7) and those determined experimentally (Table 1) indicate that a single random motional process modulates both the quadrupole interaction and the ^{27}Al–^{1}H dipolar interactions for ^{27}Al in alum. This process may dominate at low temperatures while other motional processes may become important at higher temperatures. These processes may affect the quadrupole coupling and dipolar interactions in a different manner and result in fluctuations from these interactions which become uncorrelated (Eq. (5)). In this case, identical values of T_2 will be expected for the two inner transitions and correspondingly for the two outer satellite transitions.

The T_2 values listed in Table 1 for the ^{27}Al sites **1**–**3** in principle allow determination of the correlation parameter k, the product $\overline{q^2}\tau_c$, and a value for the homogeneous linewidth, caused by uncorrelated relaxation, from a three-parameter fit to the expressions for the four different satellite transitions in Eq. (7). However, a reliable determination of these parameters could not be achieved by this method, since a least-squares fit shows that the parameters are highly correlated. This most likely reflects the simplicity of the model used to describe the differential T_2 relaxation by the quadrupolar–dipolar cross-relaxation terms in Eq. (7). Thus, this model primarily serves as a first attempt to explain the variation in T_2 values for the individual satellite transitions.

The important effect of the ^{27}Al–^{1}H dipolar interactions on the T_2 relaxation for alum is supported by the ^{27}Al MAS NMR spectrum of a deuterated sample of alum ($KAl(SO_4)_2 \cdot 12H_2O$) recorded at −76 °C and shown in Fig. 7. This spectrum illustrates a highly symmetric manifold of ssbs from the satellite transitions, which can be simulated in a convincing manner using the parameters $C_Q = 263$ kHz, $\eta_Q = 0.22$, and $\delta_{iso} = 0.7$ ppm. For this sample, we expect that the lower strength of the ^{27}Al–^{2}H as compared to the ^{27}Al–^{1}H dipolar couplings in the $Al(H_2O)_6^{3+}$ units of alum reduces the correlation of the quadrupolar and dipolar fluctuating fields, although the deuteration may in addition also slightly change the D_2O/H_2O dynamics. However, the reduced quadrupolar–dipolar cross-relaxation would result in similar T_2 values for the two inner and the two outer satellite transitions as observed by the high symmetry of the ssb manifold for $KAl(SO_4)_2 \cdot 12D_2O$ (Fig. 7).

Finally, we note that a ^{11}B MAS NMR spectrum of $NH_4B(C_6H_5)_4$, recently recorded in our laboratory [24], indicates a variation in T_2 values for the two ^{11}B ($I = 3/2$) satellite transitions for this compound, although the effect on the spectrum is less apparent when compared to the ^{27}Al MAS NMR spectra of alum

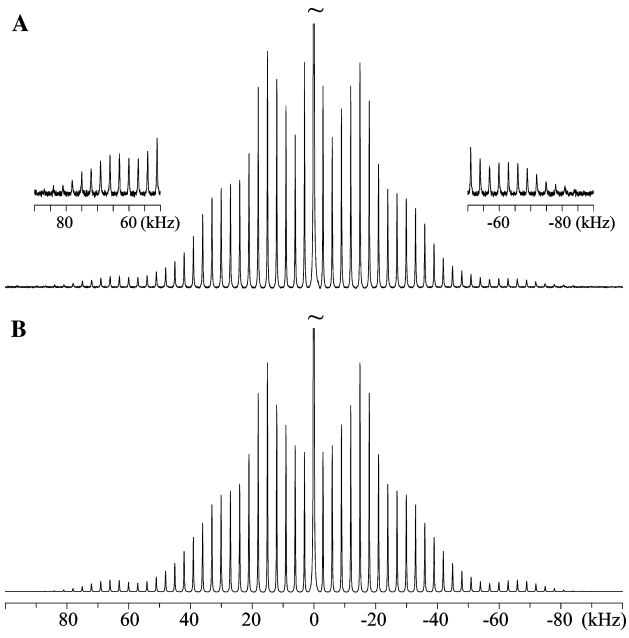

Fig. 7. (A) ^{27}Al MAS NMR spectrum (7.05 T, $\nu_r = 3.0$ kHz) of the satellite transitions for a deuterated sample of alum ($KAl(SO_4)_2 \cdot 12D_2O$) recorded at $T = -76$ °C. (B) Optimized simulation of the manifold of ssbs in (A), employing the parameters $C_Q = 263$ kHz, $\eta_Q = 0.22$, and $\delta_{iso} = 0.7$ ppm.

in Figs. 1 and 2. However, boron is situated in a highly symmetric tetrahedral arrangement in $NH_4B(C_6H_5)_4$, reflected by a very small ^{11}B quadrupole coupling ($C_Q = 29.4$ kHz [24]), and it has ^1H atoms in its nearest coordination sphere. Thus, the boron environment in $NH_4B(C_6H_5)_4$ exhibits rather similar quadrupolar and heteronuclear dipolar interactions as those for the $Al(H_2O)_6^{3+}$ units in alum, which may justify a difference in T_2 values for the two ^{11}B satellite transitions in $NH_4B(C_6H_5)_4$. ^{11}B and ^{27}Al quadrupole couplings in inorganic compounds are often one or two orders of magnitude larger than those observed for $NH_4B(C_6H_5)_4$ and alum. For these compounds the effect of the fluctuating field from the quadrupole interaction may be significantly larger than the contribution from the heteronuclear dipolar interaction. This would result in identical T_2 values for the $m = 1/2 \leftrightarrow m = 3/2$ and $m = -1/2 \leftrightarrow m = -3/2$ transitions (^{11}B and ^{27}Al) as well as for the outer satellite transitions for ^{27}Al and thereby in symmetric manifolds of ssbs from the satellite transitions, as generally observed for ^{11}B and ^{27}Al sites exhibiting larger quadrupole couplings than those observed for $NH_4B(C_6H_5)_4$ and alum. Asymmetries in the manifold of ssbs from the ^{27}Al satellite transitions, reflecting a variation in ssb linewidths, have also been observed in ^{27}Al MAS NMR spectra of the ammonium alum ($NH_4Al(SO_4)_2 \cdot 12H_2O$, $C_Q = 440$ kHz, $\eta_Q = 0.00$, and $T = 24$ °C) and for ettringite ($Ca_6[Al(OH)_6]_2(SO_4)_3 \cdot 26H_2O$, $C_Q = 360$ kHz, and $\eta_Q = 0.19$ [25]) which contain $Al(H_2O)_6^{3+}$ and $Al(OH)_6^{3-}$ units in their crystal structures, respectively. Again, this is in accord with the fact that both compounds exhibit significant ^{27}Al–^1H dipolar interactions and small ^{27}Al quadrupolar couplings.

4. Conclusions

Asymmetries in the manifold of ssbs from the satellite transitions, originating from systematic variations in ssb linewidths, have been observed in variable-temperature ^{27}Al MAS NMR spectra of alum ($KAl(SO_4)_2 \cdot 12H_2O$). From spin-echo ^{27}Al NMR experiments on a single crystal of alum, it has been demonstrated that these variations in ssb linewidths reflect the fact that the two inner ($m = 1/2 \leftrightarrow m = 3/2$ and $m = -1/2 \leftrightarrow m = -3/2$) and the two outer ($m = 3/2 \leftrightarrow m = 5/2$ and $m = -3/2 \leftrightarrow m = -5/2$) satellite transitions exhibit different T_2 values. The variation in T_2 values for the individual single-quantum transitions has been justified by a simple theoretical approach which considers the cross-correlation of local fluctuating fields from the quadrupolar coupling and the heteronuclear (^{27}Al–^1H) dipolar interactions on the T_2 values. A correlation of these fluctuating fields will result in different T_2 values for the individual ^{27}Al transitions. This fact and the observed variation in T_2 values indicate that a single random motional process modulates both the quadrupole interaction and the ^{27}Al–^1H dipolar interactions for ^{27}Al in alum at low temperatures. Variation in T_2 values for the individual transitions is expected to be observed for half-integer quadrupolar spin nuclei experiencing small quadrupole couplings and strong heteronuclear dipolar interactions. Finally, it is noted that a variation in T_2 values for the individual satellite transitions does not influence the determination of the quadrupole coupling parameters when based on least-squares fitting to integrated ssb intensities.

Acknowledgments

The use of the facilities at the Instrument Centre for Solid-State NMR Spectroscopy, University of Aarhus, sponsored by the Danish Natural Science Research Council, the Danish Technical Science Research Council, Teknologistyrelsen, Carlsbergfondet, and Direktør Ib Henriksens Fond, is acknowledged. We thank the two Danish Research Councils for financial support (J.nr. 2020-00-0018). Dr. Alexander J. Vega (DuPont Central Research and Development, Wilmingthon, Delaware, USA) and Prof. Shimon Vega (Weizmann Institute of Science, Rehovot, Israel) are acknowledged for fruitful discussions related to this study.

References

[1] H.J. Jakobsen, J. Skibsted, H. Bildsøe, N.C. Nielsen, Magic-angle spinning NMR spectra of satellite transitions for quadrupolar nuclei, J. Magn. Reson. 85 (1989) 173–180.
[2] J. Skibsted, N.C. Nielsen, H. Bildsøe, H.J. Jakobsen, Satellite transitions in MAS NMR spectra of quadrupolar nuclei, J. Magn. Reson. 95 (1991) 88–117.
[3] A. Samoson, Satellite transition high-resolution NMR of quadrupolar nuclei in powders, Chem. Phys. Lett. 119 (1985) 29–32.
[4] J. Skibsted, P. Norby, H. Bildsøe, H.J. Jakobsen, Line shapes and widths of MAS sidebands for ^{27}Al satellite transitions. Multinuclear MAS NMR of tugtupite $Na_8Al_2Be_2Si_8O_{24}Cl_2$, Solid State Nucl. Magn. Reson. 5 (1995) 239–255.
[5] J. Skibsted, N.C. Nielsen, H. Bildsøe, H.J. Jakobsen, ^{51}V MAS NMR spectroscopy: determination of quadrupole and anisotropic shielding tensors, including the relative orientation of their principal-axis systems, Chem. Phys. Lett. 188 (1992) 405–412.
[6] T. Giavani, H. Bildsøe, J. Skibsted, H.J. Jakobsen, Determination of the nitrogen chemical shift anisotropy from the second-order cross-term in ^{14}N MAS NMR spectroscopy, Chem. Phys. Lett. 377 (2003) 426–432.
[7] T. Giavani, H. Bildsøe, J. Skibsted, H.J. Jakobsen, ^{14}N MAS NMR spectroscopy and quadrupole coupling data in characterization of the IV ↔ III phase transition in ammonium nitrate, J. Phys. Chem. B 106 (2002) 3026–3032.
[8] T. Giavani, H. Bildsøe, J. Skibsted, H.J. Jakobsen, A solid-state ^{14}N magic-angle spinning NMR study of some amino acids, J. Magn. Reson. 166 (2004) 262–272.
[9] A. Kumar, R.C.R. Grace, P.K. Madhu, Cross-correlations in NMR, Prog. Nucl. Magn. Reson. Spectrosc. 37 (2000) 191–319.

[10] K. Pervushin, R. Riek, G. Wider, K. Wütrich, Attenuated T_2 relaxation by mutual cancellation of dipole–dipole coupling and chemical shift anisotropy indicates an avenue to NMR structures of very large biological macromolecules in solution, Proc. Natl. Acad. Sci. USA 94 (1997) 12366–12371.
[11] R.E. London, D.M. LeMaster, L.G. Werbelow, Unusual NMR multiplet structures of spin-1/2 nuclei coupled to spin-1 nuclei, J. Am. Chem. Soc. 116 (1994) 8400–8401.
[12] B.V. Schønwandt, H.J. Jakobsen, Phase transitions in KNO_3 studied by variable-temperature ^{15}N magic-angle spinning spectroscopy, J. Solid State Chem. 145 (1999) 10–14.
[13] A. Bielecki, D.P. Burum, Temperature-dependence of Pb-207 MAS spectra of solid lead nitrate—an accurate, sensitive thermometer for variable temperature MAS, J. Magn. Reson. Ser. A. 116 (1995) 215–220.
[14] J.L. Markley, W.J. Horsley, M.P. Klein, Spin-lattice relaxation measurements in slowly relaxing complex spectra, J. Chem. Phys. 55 (1971) 3604–3605.
[15] H. Lipson, C.A. Beevers, The crystal structure of the alums, Proc. R. Soc. (London) A 148 (1935) 664–667.
[16] A.C. Larson, D.T. Cromer, Refinement of the alum structures. III. X-ray study of the α alums, K, Rb, and $NH_4Al(SO_4)_2 \cdot 12H_2O$, Acta Cryst. 22 (1967) 793–800.
[17] G. Burns, Nuclear quadrupole coupling in the alums, J. Chem. Phys. 32 (1960) 1585–1586.
[18] N. Weiden, A. Weiss, NMR and NQR investigations of nuclear quadrupole interactions at the sites of the Me^{+} and Me^{3+} in alums $Me^{+}Me^{3+}(RO_4)_2 \cdot 12H_2O$ (R = S, Se). The electric field gradients at room temperature, Ber. Bunsenges. Phys. Chem. 78 (1974) 1031–1050.
[19] N. Weiden, A. Weiss, NMR and NQR investigations of nuclear quadrupole interactions in alums. II. Internal motions and the temperature dependence of the electric field gradient, Ber. Bunsenges. Phys. Chem. 79 (1975) 557–644.
[20] N. Weiden, A. Weiss, NMR and NQR investigations of nuclear quadrupole interactions in alums. III. The temperature dependence of the electric field gradient at the site of Me^{I} and Me^{III} in the γ-alum $NaAl(SO_4)_2 \cdot 12H_2O$, J. Magn. Reson. 20 (1975) 279–285.
[21] J. Haase, E. Oldfield, Spin-echo behaviour of nonintegral-spin quadrupolar nuclei in inorganic solids, J. Magn. Reson. A 101 (1993) 30–40.
[22] D.E. Woessner, H.K.C. Timken, The influence of MAS on spin–lattice relaxation curves and nuclear spin excitation of half-integer spin quadrupolar nuclei in solids, J. Magn. Reson. 90 (1990) 411–419.
[23] M.E. Stoll, A.J. Vega, R.W. Vaughan, Double resonance interferometry: relaxation times for dipolar forbidden transitions and off-resonance effects in an AX spin system, J. Chem. Phys. 67 (1977) 2029–2038.
[24] M.R. Hansen, T. Vosegaard, H.J. Jakobsen, J. Skibsted, ^{11}B chemical shift anisotropies in borates from ^{11}B MAS, MQMAS, and single-crystal NMR spectroscopy, J. Phys. Chem. A 108 (2004) 586–594.
[25] J. Skibsted, E. Henderson, H.J. Jakobsen, Characterization of calcium aluminate phases in cements by ^{27}Al MAS NMR spectroscopy, Inorg. Chem. 32 (1993) 1013–1027.